

# Fermilab

Performance of an Optical TPC Geant4 Simulation with Opticks  
GPU-Accelerated Photon Propagation

FERMILAB-PUB-25-0105-V

arXiv:2502.13215

This manuscript has been authored by Fermi Forward Discovery Group, LLC  
under Contract No. 89243024CSC000002 with the U.S. Department of Energy,  
Office of Science, Office of High Energy Physics.

# Performance of an Optical TPC Geant4 Simulation with Opticks GPU-Accelerated Photon Propagation

I. Parmaksiz,<sup>3</sup> K. Mistry,<sup>3</sup> E. Church,<sup>21</sup> C. Adams,<sup>2</sup> J. Asadi,<sup>3</sup>  
 J. Baeza-Rubio,<sup>19</sup> K. Bailey,<sup>2</sup> N. Byrnes,<sup>3</sup> B.J.P. Jones,<sup>3</sup> I.A. Moya,<sup>12</sup>,  
 K.E. Navarro,<sup>3</sup> D.R. Nygren,<sup>3</sup> P. Oyedele,<sup>15</sup> L. Rogers,<sup>2</sup> F. Samaniego,<sup>15</sup>,  
 K. Stogsdill,<sup>3</sup> H. Almazán,<sup>18</sup> V. Álvarez,<sup>27</sup> B. Aparicio,<sup>23</sup> A.I. Aranburu,<sup>25</sup>,  
 L. Arazi,<sup>7</sup> I.J. Arnquist,<sup>21</sup> F. Auria-Luna,<sup>23</sup> S. Ayet,<sup>20</sup> C.D.R. Azevedo,<sup>5</sup>,  
 F. Ballester,<sup>27</sup> M. del Barrio-Torregrosa,<sup>25,9</sup> A. Bayo,<sup>11</sup>,  
 J.M. Benlloch-Rodríguez,<sup>25</sup> F.I.G.M. Borges,<sup>14</sup> A. Brodolin,<sup>25,22</sup> S. Cárcel,<sup>20</sup>,  
 A. Castillo,<sup>25</sup> L. Cid,<sup>11</sup> C.A.N. Conde<sup>a</sup>,<sup>14</sup> T. Contreras,<sup>10</sup> F.P. Cossío,<sup>25,24</sup>,  
 R. Coupe,<sup>18</sup> E. Dey,<sup>3</sup> G. Díaz,<sup>26</sup> C. Echevarria,<sup>25</sup> M. Elorza,<sup>25,9</sup> J. Escada,<sup>14</sup>,  
 R. Esteve,<sup>27</sup> R. Felkai<sup>b</sup>,<sup>7</sup> L.M.P. Fernandes,<sup>13</sup> P. Ferrario<sup>c</sup>,<sup>25,8</sup> A.L. Ferreira,<sup>5</sup>,  
 F.W. Foss,<sup>4</sup> Z. Freixa,<sup>24,8</sup> J. García-Barrena,<sup>27</sup> J.J. Gómez-Cadenas<sup>d</sup>,<sup>25,8</sup>,  
 J.W.R. Grocott,<sup>18</sup> R. Guenette,<sup>18</sup> J. Hauptman,<sup>1</sup> C.A.O. Henriques,<sup>13</sup>,  
 J.A. Hernando Morata,<sup>26</sup> P. Herrero-Gómez,<sup>17</sup> V. Herrero,<sup>27</sup> C. Hervés  
 Carrete,<sup>26</sup> Y. Ifergan,<sup>7</sup> F. Kellerer,<sup>20</sup> L. Larizgoitia,<sup>25,9</sup> A. Larumbe,<sup>23</sup>,  
 P. Lebrun,<sup>6</sup> F. Lopez,<sup>25</sup> N. López-March,<sup>20</sup> R. Madigan,<sup>4</sup> R.D.P. Mano,<sup>13</sup>,  
 A.P. Marques,<sup>14</sup> J. Martín-Albo,<sup>20</sup> G. Martínez-Lema,<sup>7</sup> M. Martínez-Vara,<sup>20,25</sup>,  
 R.L. Miller,<sup>4</sup> J. Molina-Canteras,<sup>23</sup> F. Monrabal,<sup>25,8</sup> C.M.B. Monteiro,<sup>13</sup>,  
 F.J. Mora,<sup>27</sup> P. Novella,<sup>20</sup> A. Nuñez,<sup>11</sup> E. Oblak,<sup>25</sup> J. Palacio,<sup>11</sup>,  
 B. Palmeiro,<sup>18</sup> A. Para,<sup>6</sup> A. Pazos,<sup>24</sup> J. Pelegrin,<sup>25</sup> M. Pérez Maneiro,<sup>26</sup>,  
 M. Querol,<sup>20</sup> J. Renner,<sup>20</sup> I. Rivilla,<sup>25,8</sup> C. Rogero,<sup>22</sup> B. Romeo<sup>e</sup>,<sup>25</sup>,  
 C. Romo-Luque<sup>f</sup>,<sup>20</sup> V. San Nacienciano,<sup>23</sup> F.P. Santos,<sup>14</sup> J.M.F. dos Santos,<sup>13</sup>,  
 M. Seemann,<sup>25,9</sup> I. Shomroni,<sup>17</sup> P.A.O.C. Silva,<sup>13</sup> A. Simón,<sup>25</sup> S.R. Soleti,<sup>25,8</sup>,  
 M. Sorel,<sup>20</sup> J. Soto-Oton,<sup>20</sup> J.M.R. Teixeira,<sup>13</sup> S. Teruel-Pardo,<sup>20</sup> J.F. Toledo,<sup>27</sup>,  
 C. Tonnelé,<sup>25</sup> S. Torelli,<sup>25</sup> J. Torrent,<sup>25,16</sup> A. Trettin,<sup>18</sup> A. Usón,<sup>20</sup>,  
 P.R.G. Valle,<sup>25,24</sup> J.F.C.A. Veloso,<sup>5</sup> J. Waiton,<sup>18</sup> A. Yubero-Navarro,<sup>25,9</sup>

<sup>1</sup> Department of Physics and Astronomy, Iowa State University, Ames, IA 50011-3160, USA.

<sup>2</sup> Argonne National Laboratory, Argonne, IL 60439, USA.

<sup>3</sup> Department of Physics, University of Texas at Arlington, Arlington, TX 76019, USA.

<sup>4</sup> Department of Chemistry and Biochemistry, University of Texas at Arlington, Arlington, TX 76019, USA.

<sup>5</sup> Institute of Nanostructures, Nanomodelling and Nanofabrication (i3N), Universidade de Aveiro, Campus de Santiago, Aveiro, 3810-193, Portugal.

- <sup>6</sup> Fermi National Accelerator Laboratory, Batavia, IL 60510, USA.
- <sup>7</sup> Unit of Nuclear Engineering, Faculty of Engineering Sciences, Ben-Gurion University of the Negev, P.O.B. 653, Beer-Sheva, 8410501, Israel.
- <sup>8</sup> Ikerbasque (Basque Foundation for Science), Bilbao, E-48009, Spain.
- <sup>9</sup> Department of Physics, Universidad del Pais Vasco (UPV/EHU), PO Box 644, Bilbao, E-48080, Spain.
- <sup>10</sup> Department of Physics, Harvard University, Cambridge, MA 02138, USA.
- <sup>11</sup> Laboratorio Subterráneo de Canfranc, Paseo de los Ayerbe s/n, Canfranc Estación, E-22880, Spain.
- <sup>12</sup> Case Western Reserve University, Cleveland, OH 44106, USA.
- <sup>13</sup> LIBPhys, Physics Department, University of Coimbra, Rua Larga, Coimbra, 3004-516, Portugal.
- <sup>14</sup> LIP, Department of Physics, University of Coimbra, Coimbra, 3004-516, Portugal.
- <sup>15</sup> Department of Physics, University of Texas at El Paso, El Paso, TX 79968, USA.
- <sup>16</sup> Escola Politècnica Superior, Universitat de Girona, Av. Montilivi, s/n, Girona, E-17071, Spain.
- <sup>17</sup> Racah Institute of Physics, The Hebrew University of Jerusalem, Jerusalem 9190401, Israel.
- <sup>18</sup> Department of Physics and Astronomy, Manchester University, Manchester. M13 9PL, United Kingdom.
- <sup>19</sup> Wright Laboratory, Department of Physics, Yale University, New Haven, CT 06520, USA.
- <sup>20</sup> Instituto de Física Corpuscular (IFIC), CSIC & Universitat de València, Calle Catedrático José Beltrán, 2, Paterna, E-46980, Spain.
- <sup>21</sup> Pacific Northwest National Laboratory (PNNL), Richland, WA 99352, USA.
- <sup>22</sup> Centro de Física de Materiales (CFM), CSIC & Universidad del Pais Vasco (UPV/EHU), Manuel de Lardizabal 5, San Sebastián / Donostia, E-20018, Spain.
- <sup>23</sup> Department of Organic Chemistry I, Universidad del Pais Vasco (UPV/EHU), Centro de Innovación en Química Avanzada (ORFEO-CINQA), San Sebastián / Donostia, E-20018, Spain.
- <sup>24</sup> Department of Applied Chemistry, Universidad del Pais Vasco (UPV/EHU), Manuel de Lardizabal 3, San Sebastián / Donostia, E-20018, Spain.
- <sup>25</sup> Donostia International Physics Center, BERC Basque Excellence Research Centre, Manuel de Lardizabal 4, San Sebastián / Donostia, E-20018, Spain.
- <sup>26</sup> Instituto Gallego de Física de Altas Energías, Univ. de Santiago de Compostela, Campus sur, Rúa Xosé María Suárez Núñez, s/n, Santiago de Compostela, E-15782, Spain.
- <sup>27</sup> Instituto de Instrumentación para Imagen Molecular (I3M), Centro Mixto CSIC - Universitat Politècnica de València, Camino de Vera s/n, Valencia, E-46022, Spain.

<sup>a</sup>Deceased.

<sup>b</sup>Now at Weizmann Institute of Science, Israel.

<sup>c</sup>On leave.

<sup>d</sup>NEXT Spokesperson.

<sup>e</sup>Now at University of North Carolina, USA.

<sup>f</sup>Now at Los Alamos National Laboratory, USA.

### Abstract

We investigate the performance of `Opticks`, an NVIDIA `OptiX` API 7.5 GPU-accelerated photon propagation compared with a single-threaded `Geant4` simulation. We compare the simulations using an improved model of the `NEXT-CRAB-0` gaseous time projection chamber. Performance results suggest that `Opticks` improves simulation speeds by between  $58.47 \pm 0.02$  and  $181.39 \pm 0.28$  times relative to a CPU-only `Geant4` simulation and these results vary between different types of GPU and CPU. A detailed comparison shows that the number of detected photons, along with their times and wavelengths, are in good agreement between `Opticks` and `Geant4`.

**Keywords:** Photon propagation, Alpha particles, GPUs, TPC

## 1 Introduction

Time projection chambers (TPCs) generate tens to hundreds of millions of photons through primary and secondary scintillation light when charged particles in the keV to MeV energy range interact in the detector volume. The simulation of these photons, known as *optical photons*, is commonly carried out using the software package `Geant4` [1–3]. In these simulations, the photon propagation is often the largest portion of the simulation time compared with the primary particle generation, ionization electron drift, detector and physics initialization, and file writing. This is predominately due to the huge number of photons needing to be tracked through the detector geometry.

Many methods are employed to reduce simulation times with some approximations. The optical library method involves generating precomputed light tables by simulating hundreds of millions of optical photons in voxelized regions of the detector. The probability of producing a photoelectron on a sensor such as a photomultiplier tube (PMT) can then be mapped for a given energy deposition in the detector volume from a particular voxel. While this method is practical, simulation times scale with the detector volume, and it can take several weeks to produce the tables for a detector geometry. In addition, for large detectors and/or those with large numbers of sensors, file sizes can grow to huge sizes and the larger memory requirements make the use of light tables unfeasible. Other methods include the semi-analytical model [4], generative adversarial neural networks (GAN) [5] as employed by experiments including

SBND [6] and DUNE [7], and differential simulations with ML [8]. The semi-analytical model predicts (with a precision better than 10%) the amount of observed light at a photosensor using the relative positions of the energy deposition and photosensor while the GAN is trained to make predictions of the number of photons at each photodetector with 20-50 times improvement with respect to `Geant4`. Differential simulations provide flexibility with tuneable parameters from learning directly on the data to help tune the agreement between data and simulation.

In this paper, we employ the use of graphical processing units (GPUs) to propagate optical photons within a `Geant4` simulation. GPUs offer large parallelization which can rapidly speed up simulation times, accounting for physics such as reflections and wavelength shifting with minimal approximations. Furthermore, their use can supplement or replace existing simulation techniques such as the optical libraries, and be incorporated into speeding up other parts of the simulation [9]. This allows for a more convenient method for Monte Carlo productions after geometry changes, detector development, and testing. The use of GPUs to propagate photons is becoming more widespread, with projects such as `Chroma` [10] being adopted in various experiments and detector simulations [11, 12]. However, there are some limitations with using `Chroma` including no benefit from ongoing NVIDIA acceleration structure and ray tracing developments, and no use of dedicated ray tracing (RT) hardware cores in RTX GPUs.

In this work, we use the latest `Opticks` (v0.2.7) package for GPU-accelerated photon propagation for the `NEXT-CRAB-0` detector, an optical

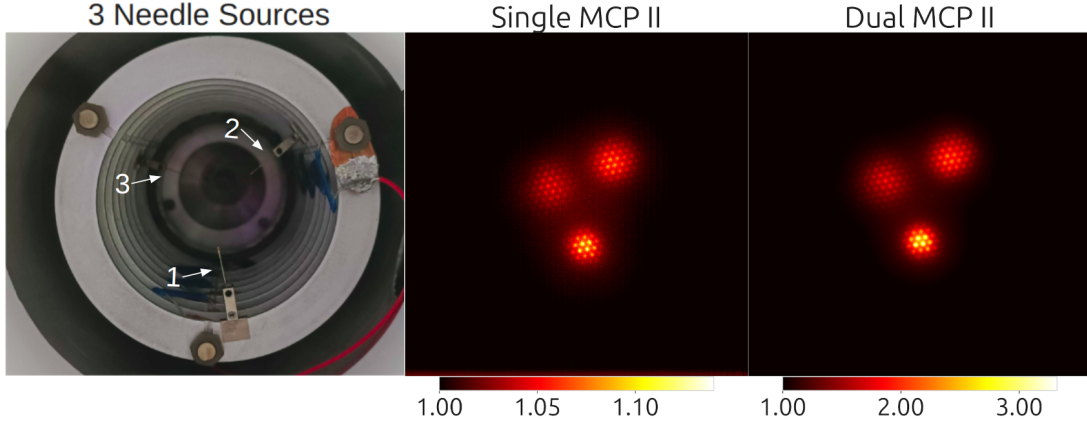


**Fig. 1** Left: the interior of the **NEXT-CRAB-0** detector. Three needle sources are shown by the thin metal rods attached to the field cage with distances 4, 10, and 14 cm from the electroluminescence region for needles 1, 2, and 3, respectively. Center and Right: Images from the **NEXT-CRAB-0** detector with Single (center) and Dual MCP II (right) at 6 bar xenon with three  $\text{Pb-210}$  alpha sources. The images contain the averaged intensities from alpha events. The color of the images is normalized to their mean.

TPC with an electron-multiplying charge-coupled device (EM-CCD) camera for imaging tracks [13]. The use of `Opticks` resolves issues related to the use of `Chroma` and is being incorporated into many detector simulations in particle physics, including JUNO [14] and LHCb-RICH [15]. It is actively being developed and has a simple interface to `Geant4` – with an example currently being integrated into the main repository [16].

We study the performance improvements with various hardware, validate sensor hits with and without the addition of `Opticks` to check its consistency with `Geant4`, and compare the images with data from the **NEXT-CRAB-0** detector.

The paper is structured as follows: in Section 2, we describe the **NEXT-CRAB-0** detector, including the latest updates to the detector. Subsequently, we detail the detector simulation in Section 3. Finally in Section 4, we show the performance speed improvements with different GPU architectures while also validating its performance with `Geant4`.

## 2 The **NEXT-CRAB-0** Detector

**NEXT-CRAB-0** is a time projection chamber with high-pressure xenon that uses a VUV-to-visible image intensifier coupled to EM-CCD to image particle tracks. The initial demonstration of this technology along with its detailed description is given in Ref. [13].

Charged particles produced in the detector ionize and excite the xenon producing an initial flash of scintillation light (S1) along with a trail of ionization electrons along the charged particle trajectory. The ionization charge drifts in an electric field towards the electroluminescence (EL) region where the ionization charge is converted in a strong electric field to a second flash of light known as the S2 signal with gains ranging from hundreds to thousands of photons per electron. To detect the xenon scintillation light ( $172 \pm 5.5$  nm [17]), the light is focused at the cathode side through a  $\text{MgF}_2$  lens into an image intensifier which further amplifies to produce photons in the visible which are detected by an EM-CCD. The detector does not require wavelength shifters such as TPB or PEN commonly used in noble gas or liquid detectors [18–21].

This work includes updates to the detector, incorporating three  $^{210}\text{Pb}$  needle sources inserted into the detector volume at three separate drift distances 4, 10, and 14 cm along the TPC axis, as shown in the left image of Figure 1. The decay chain of  $^{210}\text{Pb}$  leads to a  $^{210}\text{Po}$  daughter that alpha decays with 5.3 MeV energy. These alphas provide an excellent test of the optical simulation speeds due to the hundreds of millions of photons produced in their S1 and S2 light and are currently being studied in **NEXT-CRAB-0** for diffusion characterization in the detector.

In addition, the single microchannel plate (MCP) `photonis` image intensifier (II) that was

used in the previous study [13] has been replaced with a dual MCP **photonis II** which has up to 27 times more photon gain giving brighter images. The EL region in **NEXT-CRAB-0** consists of two photo-etched hexagonal meshes with 2.5 mm diameter hexagons and 100 micron wire widths. When the optical system is in focus, hexagonal meshes can be resolved by the EM-CCD (Figure 1). The center image shows the image using the single MCP while the brighter image on the right shows the dual MCP II.

### 3 Detector Simulation

The detector simulation uses a modified version of **Nexus** [22], a **Geant4**-based simulation framework developed by the **NEXT** Collaboration. The modifications include a modular version of **Geant4** as described in Ref. [23]. This enables the use of a uniform drift and electric field or employing the **Garfield++** package [24] to model electron drift with an imported detailed map of the electric field generated via **COMSOL** [25]. The **COMSOL** model used here includes a CAD design (via **Fusion 360** [26]) of the **NEXT-CRAB-0** geometry including realistic hexagonal meshes and field cage. **Geant4** handles the primary particle generation with energy depositions inside the detector volume. The field cage is constructed from **Fusion 360**, which is shown in Figure 2 along with the electrical fields derived from **COMSOL**. A careful description of the electric field and of the mesh is required, requiring the use of a **COMSOL** simulation to see features like the funneling of the electrons through the meshes. Alpha particles are simulated, accounting for the needle head shape which can induce geometrical effects on the alpha particle ionization cluster.

| Name                 | Version |
|----------------------|---------|
| <b>Geant4</b>        | 11.1.1  |
| <b>Opticks</b>       | 0.2.7   |
| <b>Cuda</b>          | 11.7    |
| <b>NVIDIA OptiX</b>  | 7.5     |
| <b>NVIDIA Driver</b> | 535     |
| <b>COMSOL</b>        | 6.0     |
| <b>Garfield++</b>    | 4.0     |

**Table 1** The important packages used in this simulation along with their version numbers. **Opticks** depends on **CUDA** and **NVIDIA** GPUs.

The simulation can be compiled with or without **Opticks** to propagate the scintillation photons

in order to compare the results with propagation via **Geant4**. The list of important packages and versions that are used in this paper are shown in Table 1.

**Opticks** is an open source project functional with the use of **NVIDIA** GPUs and has seamless integration with **Geant4** [14, 27]. It uses the ray tracing engine **OptiX 7.5** provided by **NVIDIA** [14, 28-30]. Geometry translation and ray generation are handled by **NVIDIA OptiX** while optical physics processes such as scattering, absorption, scintillator reemission, and boundary processes are handled by **CUDA** programs [31]. Wavelength shifting is not yet available but is currently being implemented. **Opticks** allows automatic fast geometry translation from **Geant4** to **OptiX** and with geometry conversion possible with either using a **GDML** file or **DetectorConstruction** class in **Geant4**. Comparisons of geometry translation are shown in Figure 3. Many geometry solids in **Geant4** such as cylinders and boxes are supported and more are currently in the process of being implemented such as tessellated solids. **Opticks** also accounts for any optical surfaces defined along with the material properties such as refractive index and absorption lengths and produces optical photons by scintillation and Cerenkov processes. In this work, we only use the scintillation process due to the negligible amount of Cerenkov light produced in the detector at particle energies of interest.

**Opticks** utilizes environmental variables to configure important simulation parameters, such as the maximum number of photons to simulate. A visual diagram of how **Opticks** interacts with our simulation package is shown in Figure 4. As an example, for an alpha event, **S1** and **S2** **gensteps** are collected and passed to **Opticks**. If the collected amount of photons is less than 97 % of the maximum number of photons which is defined at the beginning of the simulation, photons are simulated at the end of the event. Otherwise, they are simulated in batches. The 97% limit is chosen to avoid maxing out the video random access memory (**VRAM**) of the GPUs (listed in Table 2). After each simulation execution, the hits are collected from GPU using **SEvt::Get\_EGPU** function, and then GPU buffers are reset [14, 27, 32]. If the hit collection happens at the end of the event, it is written to a file.

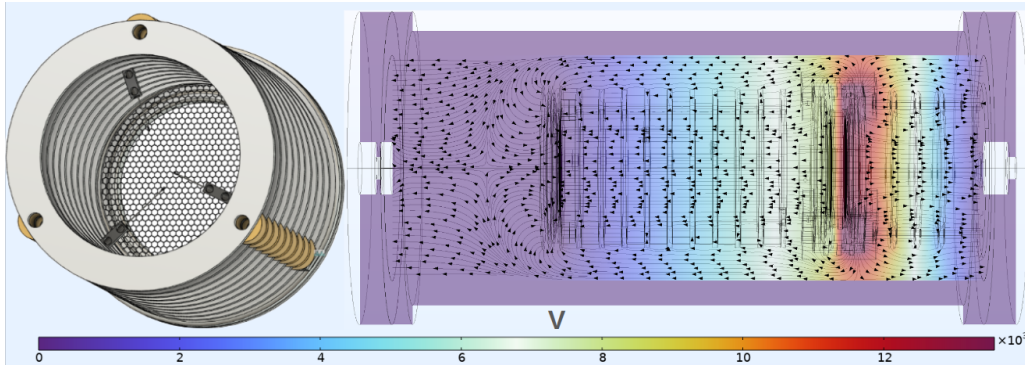


**Fig. 2** Rendering of the field cage with three needle sources from Fusion 360, and simulated electric fields and potentials from COMSOL. The gradient of electric potential is shown by the color bar while the direction of the field lines is displayed by black arrows.

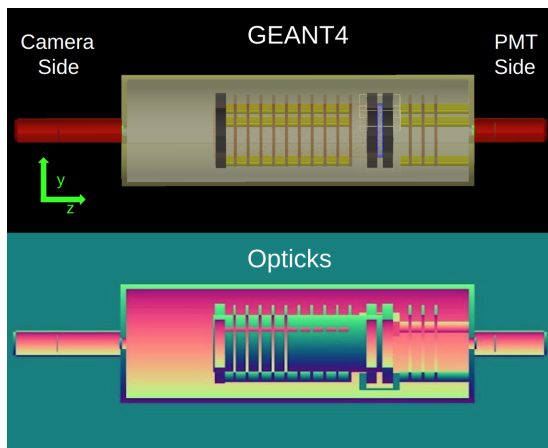


**Fig. 3** Geometry rendering of NEXT-CRAB-0 in Opticks and Geant4. The  $z$  direction points along the drift axis (with  $z = 0$  closest to the electroluminescence region), while the  $x$  and  $y$  coordinates are perpendicular to this.

## 4 Simulation Comparisons

Several comparisons are performed between Geant4 and Opticks where the speed with different computer architectures and simulation agreements are compared.

### 4.1 Performance

The performance of Opticks across different computer systems with varying memory and processors is investigated. We compare the single thread performance of Geant4 photon propagation with photons propagated via a single GPU and Opticks. Table 2 details the different computer systems used.

Between 15 and 154 million (M) photons are simulated by generating 500 alpha particles with

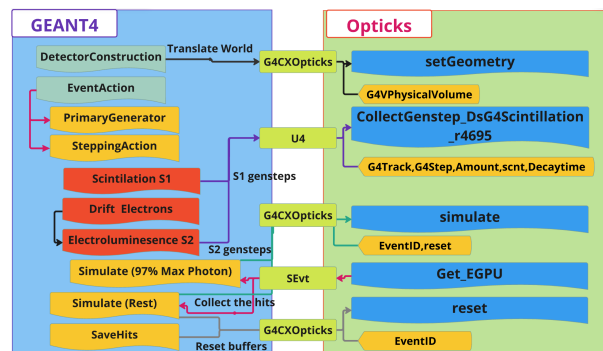


**Fig. 4** Flowchart of the simulation of an event. The figure contains the class names responsible for geometry translation to the collection of hits. The direction of information flow between Opticks and Geant4 is indicated by arrows.

| GPU (RTX) | Max Photon(M) | VRAM (GB) | Release Date |
|-----------|---------------|-----------|--------------|
| 3050-Ti M | 26            | 4         | 05/11/2021   |
| 2060      | 45            | 6         | 01/15/2019   |
| 3060-Ti   | 60            | 8         | 12/01/2020   |
| 4090      | 160           | 24        | 12/10/2022   |

**Table 2** The various GPUs studied with their available VRAM and the max number of photons batch size configured to optimize speed.

energy ranges of 0.5 MeV to 5.3 MeV at 10 bar xenon placed in the center of the drift region. Each alpha event produces about 25,510 photon(ph)/MeV in S1 light, about 45,454 electron(e)/MeV total ionization charge. The ionization electrons are amplified in the EL region with a gain of 640 ph/e. The total S1 and S2 photons can reach up to 154 million for a 5.3 MeV alpha energy. The time difference between the start and

end of an alpha event was recorded excluding the loading and file writing times in this comparison.

The performances are shown in log-scale in Figure 5 where it can be seen that the GPU performance is better by about a factor  $58.47 \pm 0.02$  to  $181.39 \pm 0.28$  depending on which CPU and GPU are used. These results are comparable to the recent performance result that was measured with the CaTs project, an `Opticks` example implementation in the main `Geant4` project [16, 33]. By comparing the slopes between the desktop GPUs RTX 20, RTX 30, and RTX 40 series, it is observed that there is an average factor of  $2.09 \pm 0.36$  speed up from one generation to the next. Due to the power limitations of laptop GPUs and reduced clock speeds, the RTX-3050-Ti M speeds are close to the RTX-2060. The speed improvements come from the fact that each new RTX series of GPUs is better optimized for ray tracing, has more ray tracing cores, and has higher clock speeds. The combination of improved GPU and CPU performance contributes to the factor of 3 speed that is seen in Table 3.

The partitioning of time spent between particle generation and ionization electron drifts compared with the optical photon propagation is also compared. We simulated 10 alpha events between 0.5 to 5.3 MeV energies with and without photon propagation for each device. Then, using the same energy alpha events, we obtained the ratios of the total event time without photon propagation to the ones with photon propagation. The mean and standard deviation of the results from CPU-only events across all devices are calculated to be  $0.16 \pm 0.01\%$ . Meanwhile, for events that utilize `Opticks` for photon propagation, we find this ratio to be  $15.49 \pm 7.24\%$ . As expected, the photon propagation dominates the simulation time, but this proportion is reduced dramatically with the introduction of `Opticks`.

## 4.2 Simulation Agreement

The number of detected S1 and S2 photons are compared between `Opticks`, and `Geant4` at the camera and PMT in NEXT-CRAB-0 as labeled in Figure 3. Both sensors are modeled as circular disks, and we use a uniform electric field in these comparisons as described in Ref. [13]. We set the efficiency of the photodetectors to 1 and simulated 2000 alpha particles with 5.3 MeV energy on the

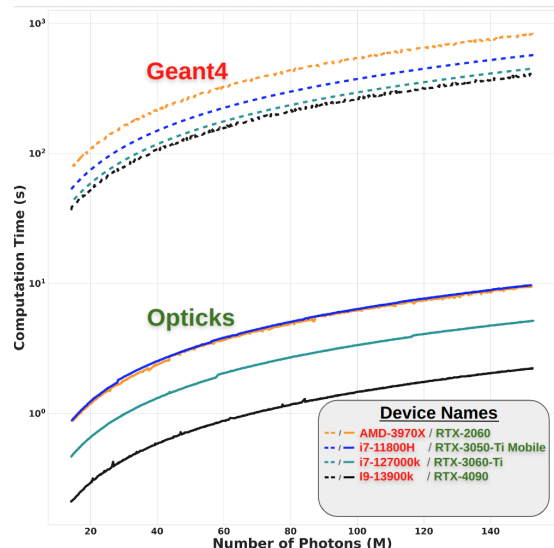


**Fig. 5** Performance comparison between `Geant4` and `Opticks` using different CPU (AMD/i7/i9 devices) and GPU (RTX devices) combinations. The ratios are given in Table 3.

| Device Names            | GPU/CPU Ratio     |
|-------------------------|-------------------|
| RTX-3050-Ti M/i7-11800H | $58.47 \pm 0.02$  |
| RTX-2060/AMD-3970X      | $86.67 \pm 0.13$  |
| RTX-3060-Ti/i7-12700k   | $86.52 \pm 0.06$  |
| RTX-4090/i9-13900k      | $181.39 \pm 0.28$ |

**Table 3** CPU and GPU performance ratios for each computer. The slopes are estimated by a linear fit to each curve in Figure 5. The ratios are calculated using the reciprocal slopes (photons/second), where the `Opticks` (GPU) result is divided by the `Geant4` (CPU) one. The uncertainties are given by the error on the line fit and propagated to the ratio.

side of the field cage. Counts are compared with and without reflections on material surfaces using the i9-12900k CPU and RTX-4090 GPU.

Figure 6 shows the  $x$  coordinate of detected S2 photons at the camera and PMT planes, histogrammed over all events with reflections for `Geant4` and `Opticks`. The distributions of the  $y$  coordinate points are similar. We find good agreement in the camera plane, while there is a small difference at the edges of the PMT plane, potentially due to differences in the reflected light between the simulations.

To investigate this further, we examine the agreement with and without reflections turned on at the camera and PMT for S1 and S2 light. The distributions of photon numbers over the 2000 alpha events are fit to a Gaussian distribution and



their means and standard deviations are reported in Table 4. We find that the number of detected S1 and S2 photons is in agreement for **Geant4** and **Opticks** without reflections. However, a larger difference between the simulations is observed when reflections are included.

When including reflections, the largest difference in the mean is in the S1 light detected at the PMT of 32%. The S2 at the PMT and S1 and S2 at the camera are in agreement to 2% or lower. Without reflections, the S1 agreement in the mean improves to within 3%, while the S2 at the PMT and S1 and S2 at the camera are in agreement to within a percent.

These comparisons indicate that the disagreement may be due to how each simulation handles the photon reflections, potentially due to the geometry conversion.

#### With Reflections

|                | PMT  |             | Camera |           |
|----------------|------|-------------|--------|-----------|
|                | S1   | S2          | S1     | S2        |
| <b>Geant4</b>  | 45±7 | 169013±1048 | 40±6   | 24954±173 |
| <b>Opticks</b> | 66±9 | 170219±1300 | 41±6   | 25492±180 |

#### No Reflections

|                | PMT  |             | Camera |           |
|----------------|------|-------------|--------|-----------|
|                | S1   | S2          | S1     | S2        |
| <b>Geant4</b>  | 44±6 | 162132±1533 | 38±7   | 22895±154 |
| <b>Opticks</b> | 44±7 | 162820±1371 | 39±6   | 23081±159 |

**Table 4** The mean number of photons detected at the PMT and camera for S1 and S2 photons. The top table includes reflections, while the bottom table removes reflections from the simulation. The uncertainties are the one-sigma values from Gaussian fits of the photon distribution.

Comparisons of the wavelength and the timing constants of the S1 and S2 light were also done. We found that the wavelength agreement was within 0.4%. The distribution of the S1 photon arrival times was fitted with a sum of two exponential decays, accounting for the fast and slow scintillation time constants in gaseous xenon. This was found to be within 4.5% for the fast component and 0.5% for the slow component. The mean S2 arrival times are in agreement to within a fraction of a percent (see Figure 7).

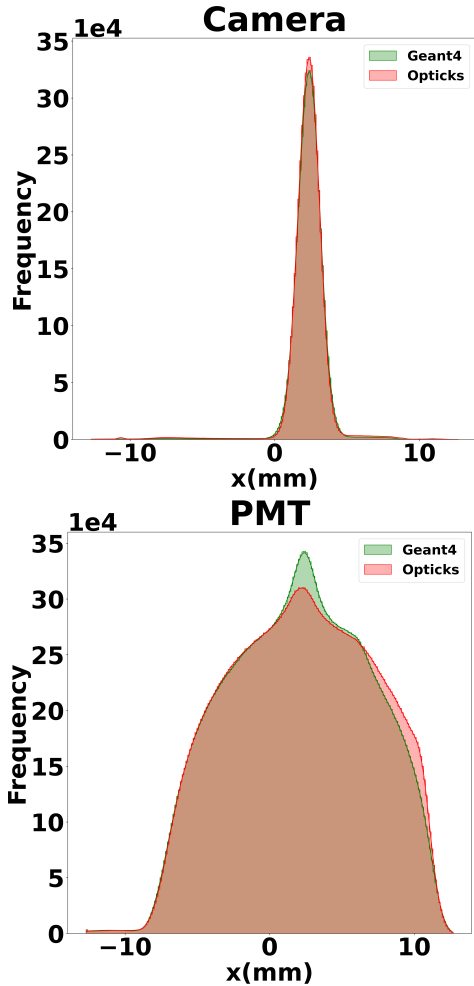


**Fig. 6** Distribution of  $x$  coordinate points of detected S2 photons for the camera (top) and PMT (bottom) planes, simulated using **Geant4** and **Opticks**.

### 4.3 Data and Simulation

A comparison of the images at the camera taken with 8 bar xenon is shown in Figure 8. The simulations via **Geant4** and **Opticks** give images that are strikingly similar to the data. The hexagonal shapes in the images are obtained due to the funneling of the ionization electrons through the hexagonal mesh. This feature is obtained through the detailed model of the electric field lines and electron drift via **Garfield++** and **COMSOL**. The oblong shape of the upper right alpha image is due to distortion from the needle and the simulation has a slightly different mesh rotation compared with the data. The data appears to have an additional blurring around the alphas, which

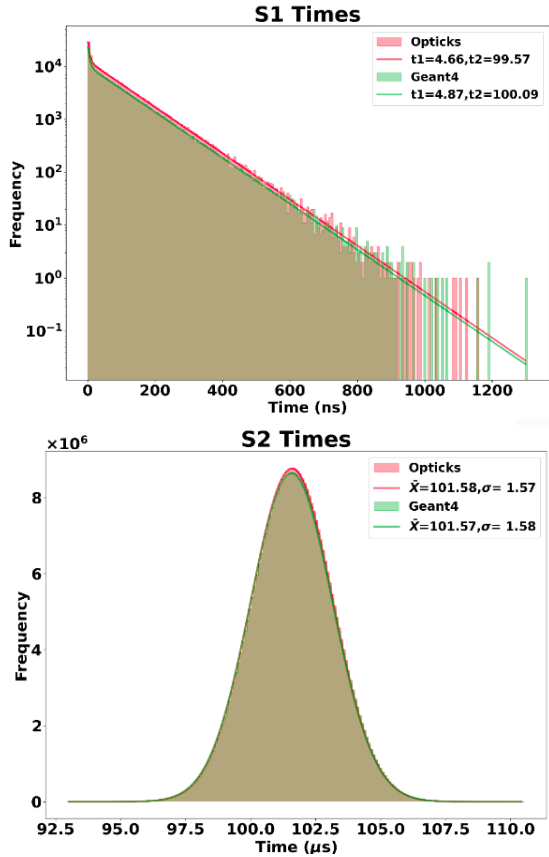


**Fig. 7** Distributions of arrival times for S1 (top) and S2 (bottom) photons. The  $t_1$  and  $t_2$  correspond to the fitted fast and slow scintillation times respectively. The  $\bar{X}$  and  $\sigma$  indicate the mean and standard deviation of the S2 photon arrival times.

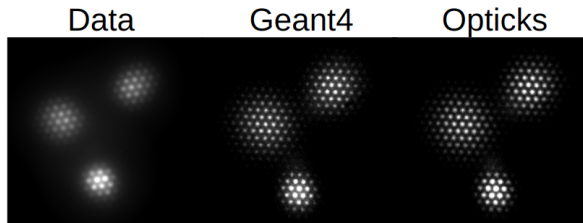


**Fig. 8** Comparisons of the average image of 5.3 MeV alpha particles recorded by the NEXT-CRAB-0 detector with Geant4 and Opticks.

is under investigation. With these fine detailed images, measurements of the transverse diffusion are possible and will be the subject of a future paper.

## 5 Summary

In summary, we have compared the performance of Opticks, an NVIDIA OptiX API 7.5 GPU-accelerated photon propagation compared with a single-threaded Geant4 simulation. From these results, we find that Opticks improves simulation speeds ranging from  $58.47 \pm 0.02$  to  $181.39 \pm 0.28$  over Geant4 depending on the computational specifications. Performance improves with the generation of GPUs and from one generation to the next, an average of  $2.09 \pm 0.35$  factor speed improvements is observed. Comparison of S1 and S2 response of Opticks to Geant4 shows that detection wavelengths, and times agree. We also find that the total photon hits are in good agreement when reflections are not involved. Larger differences with reflections remain under investigation.

**Acknowledgments.** The authors extend their sincere appreciation to Simon Blyth for his assistance regarding the Opticks package. The NEXT Collaboration acknowledges support from the following agencies and institutions: the European Research Council (ERC) under Grant Agreement No. 951281-BOLD; the European Union’s Framework Programme for Research and Innovation Horizon 2020 (2014–2020) under Grant Agreement No. 957202-HIDDEN; the MCIN/AEI of Spain and ERDF A way of making Europe under grants PID2021-125475NB and RTI2018-095979, and the Severo Ochoa and María de Maeztu Program grants CEX2023-001292-S, CEX2023-001318-M and CEX2018-000867-S; the Generalitat Valenciana of Spain under grants PROMETEO/2021/087 and CISEJI/2023/27; the Department of Education of the Basque Government program non-doctoral research personnel; the Spanish la Caixa Foundation (ID 100010434) under fellowship code LCF/BQ/PI22/11910019; the Portuguese FCT under project UID/FIS/04559/2020 to fund the activities of LIBPhys-UC; the Israel Science Foundation (ISF) under grant 1223/21; the Pazy Foundation (Israel) under grants 310/22, 315/19 and 465; the US Department of Energy under contracts number DE-AC02-06CH11357 (Argonne National Laboratory), DE-AC02-07CH11359 (Fermi National Accelerator Laboratory), DE-FG02-13ER42020

(Texas A&M), DE-SC0019054 (Texas Arlington) and DE-SC0019223 (Texas Arlington); the US National Science Foundation under award number NSF CHE 2004111; the Robert A Welch Foundation under award number Y-2031-20200401. Finally, we are grateful to the Laboratorio Subterráneo de Canfranc for hosting and supporting the NEXT experiment.

## References

- [1] Allison, J., *et al.*: Geant4 developments and applications. *IEEE Transactions on Nuclear Science* **53**(1), 270–278 (2006) <https://doi.org/10.1109/TNS.2006.869826>
- [2] Allison, J., *et al.*: Recent developments in geant4. *Nuclear Instruments and Methods in Physics Research Section A: Accelerators, Spectrometers, Detectors and Associated Equipment* **835**, 186–225 (2016) <https://doi.org/10.1016/j.nima.2016.06.125>
- [3] Agostinelli, S., *et al.*: Geant4 - a simulation toolkit. *Nuclear Instruments and Methods in Physics Research Section A: Accelerators, Spectrometers, Detectors and Associated Equipment* **506**, 250–303 (2003) [https://doi.org/10.1016/S0168-9002\(03\)01368-8](https://doi.org/10.1016/S0168-9002(03)01368-8)
- [4] Garcia-Gamez, D., Green, P., Szelc, A.M.: Predicting transport effects of scintillation light signals in large-scale liquid argon detectors. *The European Physical Journal C* **81**(4), 349 (2021) <https://doi.org/10.1140/epjc/s10052-021-09119-3>
- [5] Mu, W., Himmel, A.I., Ramson, B.: Photon detection probability prediction using one-dimensional generative neural network (2021). <https://arxiv.org/abs/2109.07277>
- [6] SBND Collaboration: Scintillation light in SBND: simulation, reconstruction, and expected performance of the photon detection system. *The European Physical Journal C* **84**(1046) (2024) <https://doi.org/10.1140/epjc/s10052-024-13306-3>
- [7] DUNE Collaboration: DUNE Offline Computing Conceptual Design Report (2022) [arXiv:2210.15665](https://arxiv.org/abs/2210.15665) [physics.data-an]
- [8] Lei, M., *et al.*: Implicit Neural Representation as a Differentiable Surrogate for Photon Propagation in a Monolithic Neutrino Detector (2022). <https://arxiv.org/abs/2211.01505>
- [9] Abud, A.A., *et al.*: Highly-parallelized simulation of a pixelated lartpc on a gpu. *Journal of Instrumentation* **18**(04), 04034 (2023) <https://doi.org/10.1088/1748-0221/18/04/P04034>
- [10] Seibert, S., Latorre, A.: Fast optical monte carlo simulation with surface-based geometries using chroma. (2011). [https://www.tlatorre.com/chroma/\\_downloads/chroma.pdf](https://www.tlatorre.com/chroma/_downloads/chroma.pdf)
- [11] Benjamin, J.A., Land, Naugle, S., Klein, J.: Chroma photon ray tracer for large-scale detectors. (2020). <https://www.snowmass21.org/docs/files/summaries/CompF/SNOWMASS21-CompF2-CompF0-NF10-NF0-Chroma-045.pdf>
- [12] Althueser, L., *et al.*: The nu-ball2 spectrometer at alto: experimental campaign of 2019 and perspectives for 2021. *Journal of Instrumentation* **17**, 07018 (2022) <https://doi.org/10.1088/1748-0221/17/07/P07018>
- [13] N.K. Byrnes: NEXT-CRAB-0: a high pressure gaseous xenon time projection chamber with a direct VUV camera based readout. *JINST* (2023)
- [14] Blyth, Simon C.: Opticks: Gpu optical photon simulation via nvidia optix. *EPJ Web of Conf.* **295**, 11014 (2024) <https://doi.org/10.1051/epjconf/202429511014>
- [15] Li, Y., Davis, A., Easo, S., *et al.*: Gpu-based optical photon simulation for the lhcb rich 1 detector. *European Physical Journal C* **83**(1036) (2023) <https://doi.org/10.1140/epjc/s10052-023-12158-7>
- [16] Wenzel, Hans, Yung Jun, Soon, Genser, Krzysztof, De Figueiredo, Felipe: Cats: Integration of geant4 and opticks. *EPJ Web of Conf.* **295**, 11004 (2024) <https://doi.org/10.1051/epjconf/202429511004>

- [17] Borovich, B.L., Zuev, V.S., Stavrovskii, D.B.: A contribution to the problem of an optically pumped ultraviolet xe2 laser: photoluminescence spectrum and quantum efficiency of gaseous xenon. *Soviet Journal of Quantum Electronics* **4**(9), 1138 (1975) <https://doi.org/10.1070/QE1975v004n09ABEH011556>
- [18] Yahlali, N., Garcia, J.M., Díaz, J., Soriano, A., Fernandes, L.M.: Ageing studies of tpb in noble gas detectors for dark matter and neutrinoless  $\beta\beta$  decay searches. *Spectrochimica Acta Part A: Molecular and Biomolecular Spectroscopy* **172**, 109–114 (2017) <https://doi.org/10.1016/j.saa.2016.04.025>
- [19] Asaadi, J., Jones, B.J.P., Tripathi, A., Parmaksiz, I., Sullivan, H., Williams, Z.G.R.: Emanation and bulk fluorescence in liquid argon from tetraphenyl butadiene wavelength shifting coatings. *Journal of Instrumentation* **14**(02), 02021 (2019) <https://doi.org/10.1088/1748-0221/14/02/P02021>
- [20] Domine, A., al.: Direct comparison of pen and tpb wavelength shifters in a liquid argon detector. *European Physical Journal C* **81**, 1–10 (2021) <https://doi.org/10.1140/epjc/s10052-021-09870-7>
- [21] Abraham, Y., Asaadi, J., Basque, V., Castiglioni, W., Dorrill, R., Febbraro, M., Hackett, B., Kelsey, J., Littlejohn, B.R., Parmaksiz, I., Rooks, M., Szelc, A.M.: Wavelength-shifting performance of polyethylene naphthalate films in a liquid argon environment. *Journal of Instrumentation* **16**(07), 07017 (2021) <https://doi.org/10.1088/1748-0221/16/07/P07017>
- [22] Parmaksiz, I.: Nexus Opticks Integration Repo. GitHub (2023). <https://github.com/ilkerparmaksiz/nexus/tree/Opticks>
- [23] Pfeiffer, D., De Keukeleere, L., Azevedo, C., Belloni, F., Biagi, S., Grichine, V., Hayen, L., Hanu, A.R., Hřivnáčová, I., Ivanchenko, V., Krylov, V., Schindler, H., Veenhof, R.: Interfacing geant4, garfield++ and degrad for the simulation of gaseous detectors. *Nuclear Instruments and Methods in Physics Research Section A: Accelerators, Spectrometers, Detectors and Associated Equipment* **935**, 121–134 (2019) <https://doi.org/10.1016/j.nima.2019.04.110>
- [24] Garfield++ Collaboration: Garfield++. Simulation software for gaseous detectors (2024). <https://garfieldpp.web.cern.ch/>
- [25] Edmund J.F. Dickinson, Henrik Ekström, Ed Fontes: Comsol multiphysics®: Finite element software for electrochemical analysis. a mini-review. *Electrochemistry Communications* **40**, 71–74 (2014)
- [26] Autodesk Inc.: Autodesk Fusion 360. Computer-aided design software (2024). <https://www.autodesk.com/products/fusion-360/overview>
- [27] Blyth, S.: Opticks bitbucket Repo. <https://simoncblyth.bitbucket.io/>
- [28] Blyth, Simon: Meeting the challenge of juno simulation with opticks: Gpu optical photon acceleration via nvidia® optix™. *EPJ Web Conf.* **245**, 11003 (2020) <https://doi.org/10.1051/epjconf/202024511003>
- [29] Blyth, Simon: Opticks : Gpu optical photon simulation for particle physics using nvidia® optix™. *EPJ Web Conf.* **214**, 02027 (2019) <https://doi.org/10.1051/epjconf/201921402027>
- [30] Blyth, Simon: Integration of juno simulation framework with opticks: Gpu accelerated optical propagation via nvidia® optix™. *EPJ Web Conf.* **251**, 03009 (2021) <https://doi.org/10.1051/epjconf/202125103009>
- [31] Blyth, S.C.: Opticks: Gpu optical photon simulation for particle physics using nvidia optix. *Journal of Physics: Conference Series* **898**(4), 042001 (2017) <https://doi.org/10.1088/1742-6596/898/4/042001>
- [32] Blyth, S.C.: Integration with New Opticks Using G4CXOpticks and U4. Accessed: 2024-11-07 (2024). [https://bitbucket.org/simoncblyth/opticks/src/master/docs/integration\\_with\\_new\\_opticks\\_](https://bitbucket.org/simoncblyth/opticks/src/master/docs/integration_with_new_opticks_)

[using\\_G4CXXOpticks\\_and\\_U4.rst](#)

- [33] Wenzel, H.: CaTs Repo.  
<https://github.com/hanswenzel/CaTS>